JACS
JOURNAL OF THE AMERICAN CHEMICAL SOCIETY
pubs.acs.org/JACS

Article

Sorbent Mediated Electrocatalytic Reduction of Dilute CO_2 to Methane

Jared S. Stanley, Hunter N. Pauker, Erin Kuker, Vy Dong, Robert J. Nielsen,* and Jenny Y. Yang*

Cite This: J. Am. Chem. Soc. 2025, 147, 16099−16106

Read Online

ACCESS | Metrics & More | Article Recommendations | Supporting Information

ABSTRACT: Efficient CO_2 utilization is a critical component of closing the anthropogenic carbon cycle. Most studies have focused on the use of pure streams of CO_2. However, CO_2 is generally available only in dilute streams, which requires capture by sorbents followed by energy-intensive regeneration to release concentrated CO_2. Direct utilization of sorbed-CO_2 avoids the costly regeneration step, and the sorbent-CO_2 interaction can kinetically activate CO_2 to tune its reactivity toward products that could otherwise be inaccessible with direct CO_2 reduction. We demonstrate that an *N*-heterocyclic carbene, 1,3-bis(2,6-diisopropylphenyl)imidazol-2-ylidene (DPIy), quantitatively reacts with CO_2 from dilute streams (0.04 and 10%) to form the sorbent-CO_2 substrate 1,3-bis(2,6-diisopropylphenyl)imidazolium-2-carboxylate (DPICx). Electrocatalyst iron tetraphenylporphyrin chloride (Fe(TPP)Cl) typically reduces CO_2 to CO; however, with DPICx as the substrate, the eight-electron reduced product methane (CH_4) is produced with a high Faradaic efficiency (>85%) and regeneration of the sorbent DPIy. In addition to the overall energy and capital advantages of integrated CO_2 capture and conversion, this result illustrates how sorbents can serve a dual purpose for both CO_2 capture and chemical auxiliary purposes to access unique products. CO_2 has a spectrum of reactivity with different types of sorbents; thus, these studies demonstrate how sorbent-CO_2 interactions can be leveraged for integrated capture and utilization platforms to access a wider range of CO_2-derived products.

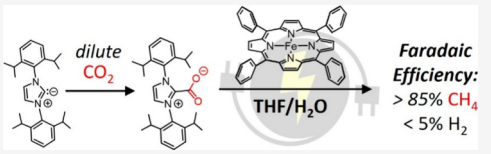

INTRODUCTION

The use of carbon dioxide (CO_2) from dilute streams is a critical barrier to closing the anthropogenic carbon cycle. Most studies that transform this C1-building block rely upon concentrated CO_2.[1,2] Capture of CO_2 from air or point sources can be achieved by various sorbents, but energy-intensive heating is required to regenerate the sorbent and release CO_2 in concentrated streams. In direct air capture (DAC), sorbent regeneration requires an estimated 75% of the capital expense and 95% of the energetic cost.[3] To address this challenge, integrated capture and conversion has emerged as an attractive route where sorbed-CO_2 (or captured-CO_2) is directly transformed to eliminate the need for CO_2 regeneration from the sorbent.[4] Toward this goal, we report a Fe-catalyzed reduction of captured-CO_2 that produces methane gas with high selectivity (Faradaic efficiency). This study features an electrocatalyst derived from the earth's most abundant transition metal and a readily available and tunable sorbent capable of CO_2 capture from air-relevant concentrations.

A key aspect of this work is that the sorbent performs a dual role in capturing CO_2 from dilute streams and as a chemical auxiliary to access a C-reduced product that would otherwise be challenging when using CO_2 as the substrate. An *N*-heterocyclic carbene (NHC) was selected as the sorbent because this class of compounds has several attractive properties for this application. They are strong nucleophiles that reversibly react with CO_2 with binding constants that can exceed what is necessary for capture from air ($K_{CO2} > 10^7$).[5,6] Their binding interaction transforms linear CO_2 into a polar and bent carboxylate that is kinetically activated toward further reactivity.[7] They are also generally resistant to reduction and therefore compatible with electrocatalytic conditions. NHCs form net neutral zwitterions upon their reaction with CO_2 instead of the anionic carboxylates common in other CO_2 sorbents (hydroxides and amines) that can inhibit the substrate approach to reducing catalytic sites.[8] Furthermore, NHCs can be synthetically tuned to modify their σ- and π-interactions with CO_2, which influence their subsequent reactivity.[9] NHCs have demonstrated use as organocatalysts for CO_2 reduction to C1 products, albeit requiring the use of stoichiometric oxygen atom acceptors.[10,11] Although NHCs and NHC carboxylates are resistant to direct reduction, they have been explored as substrates for electrochemical CO_2 reduction[12] and have been suggested as a possible substrate in imidazolium-based ionic liquid-mediated CO_2 reduction.[13,14]

Our studies focused on the use of *N*-heterocyclic carbene 1,3-bis(2,6-diisopropylphenyl)imidazol-2-ylidene (DPIy) as the sorbent and auxiliary, which forms 1,3-bis(2,6-diisopropylphenyl)imidazolium-2-carboxylate (DPICx) upon

Received: December 20, 2024
Revised: April 17, 2025
Accepted: April 18, 2025
Published: May 6, 2025

https://doi.org/10.1021/jacs.4c18303
J. Am. Chem. Soc. 2025, 147, 16099−16106

reaction with CO_2. Both compounds are commercially available. A prior computational study determined that the free energy of CO_2 binding (ΔG) in DMSO is favorable (−4.5 kcal/mol under standard conditions).[6] An analytical study on NHC carboxylates indicates that decarboxylation is more facile when larger functionalities, such as the diisopropylphenyls used here, are present on the nitrogen atoms that tilt the carboxylate out of the plane of the imidazolium.[5] This feature is important for the subsequent functionalization of CO_2.

In this work, we explored the catalytic reduction of the CO_2-bound species DPICx with the abundant metal electrocatalyst Fe(TPP)Cl, which has well-documented activity toward the selective reduction of CO_2 to CO.[15,16] However, instead of forming the 2 e^- product CO, the reduction of DPICx results in the 8 e^- reduced product CH_4 with over 85% Faradaic efficiency (FE), confirming the role of the sorbent in steering the product of the CO_2 reduction. Furthermore, regeneration of the parent NHC (DPIy, Chart 1) and catalyst stability was

Chart 1. Structures of Fe(TPP)Cl, DPIy, and DPICx

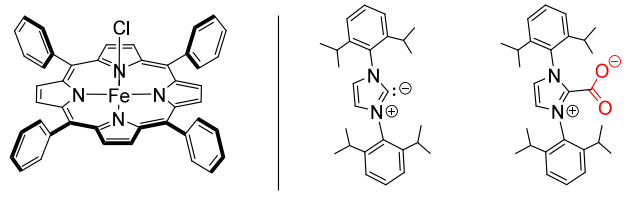

demonstrated. DPIy was also used as a sorbent for the reduction of dilute streams of CO_2 with concentrations relevant from flue gas (10%) to air (0.04%) while maintaining the high Faradaic efficiency for CH_4. CO_2 electroreduction with high selectivity (>85%) for CH_4 is rare with heterogeneous catalysts, with only a few examples.[17−20] CH_4 is also uncommon for CO_2 reduction by homogeneous catalysts,[21,22] although it has been observed as a product of CO reduction,[23] and photolytic CO_2 reduction with iron-porphyrin catalysts.[24] Furthermore, water is used as the proton source. Thus, the use of renewable electricity in this process results in carbon-neutral methane. To probe potential reaction pathways, computational and experimental studies were performed to provide evidence of potential intermediates.

The divergent reactivity from free CO_2 compared to when it is bound to a sorbent illustrates how the interaction of the latter can serve a dual purpose in both capturing CO_2 and directing the subsequent reactivity of the captured-CO_2. There are only a few studies that have explored the use of dilute CO_2 streams with molecular electrocatalysts.[25,26] Additionally, experimental studies describe how CO_2 sorbents can modify the mechanism or product in CO_2 reduction that has only been described for a few catalytic systems.[27,28] This study presents an example of the reduction of dilute CO_2 streams, down to air-relevant concentrations, and provides mechanistic and catalytic insights toward the ultimate goal of transforming carbon dioxide from dilute streams into fuels and commodity chemicals.

RESULTS

Electrolytic Studies. Our initial controlled potential electrolysis (CPE) with Fe(TPP)Cl and DPICx as substrates was conducted with THF as the solvent and H_2O as the proton source. Fe(TPP)Cl (1 mM), 20 mM DPICx, and 60 mM H_2O with 0.1 M n-Bu_4NPF_6 in THF were electrolyzed for up to 63 h at −2.35 V vs $[Fe(C_5H_5)_2]^{+/0}$. Electrolysis over this time period corresponds to an unoptimized turnover of 6, but we expect this is a lower limit as the postelectrolysis analysis of the solution demonstrates retention of the catalyst (Figure 2, *vide infra*). Under these conditions, CH_4 is formed with 86.1 ± 5% Faradaic efficiency, with 4 ± 3% H_2 (Table 1) as measured by

Table 1. Controlled Potential Electrolysis Results of Possible Intermediate Structures (20 mM) with Fe(TPP)Cl (1 mM)[c]

substrate	FE CH_4	FE H_2
DPICx (no catalyst)	0%	0%
DPICx (−1.7 V)[a]	0%	0%
DPICx	86.1 ± 5%	4 ± 3%
DPICx from 10:90 CO_2:N_2 + DPIy	92.5 ± 2.1%	3.3 ± 1%
DPICx from 0.04:99.96 CO_2:N_2 + DPIy	94.5 ± 0.7%	0.6 ± 0.8%
proposed intermediates with Fe(TPP)Cl [result with no catalyst]		
[n-Bu_4N][HCOO]	68.6 ± 6.2% [0%]	6.2 ± 3.5% [0%]
HCOOH[b]	39.9% [0%]	55.4% [94%]
HCHO (0.13 M H_2O)	32.2 ± 7.0% [0%]	9.0 ± 3.1% [0%]
CH_3OH	26.1 ± 4.1% [0%]	4.2 ± 3.3% [0%]
DPI-CH_2OH	11.3 ± 4.9% [0%]	0.33 ± 0.66% [0%]
DPI-CH_3	17.1 ± 4.0% [8.8%]	51.8 ± 8.8% [2.1%]

[a]Potential for $Fe(TPP)^{0/-1}$. [b]HCOOH is not expected to form under catalytic conditions as the solution is insufficiently acidic. [c]All CPEs were performed at −2.35 V vs $Fe(C_5H_5)_2^{+/0}$ in 0.1 M n-Bu_4NPF_6 in THF with 60 mM H_2O unless otherwise indicated. Errors represent standard deviations.

gas chromatography (GC). We note that in all of our Faradaic efficiency calculations, we only subtract 1 equiv of charge to reduce the Fe(III)(TPP)Cl to Fe(TTP), although post-electrolysis analysis by UV-visible spectroscopy indicates that most of the catalyst remains in the fully reduced form ($[Fe(TPP)]^{2-}$, Figure 2, *vide infra*). Thus, our Faradaic efficiencies for the product are potentially underestimated by up to a few percentage points. Details on the Faradaic efficiency calculations are provided in the Supporting Information. No other products are detected by GC or ^1H NMR spectroscopy. The charge passed over a representative time with a catalyst (blue) and without a catalyst (black) under otherwise identical conditions is shown in Figure 1. When no catalyst is present, minimal charge is passed, and no liquid- or gas-phase C-based products or H_2 are detected by ^1H NMR spectroscopy or GC (Figure 1, black trace).

Upon completion of the electrolysis, the solution was examined via UV-visible spectroscopy. The resulting absorbance spectrum (black trace, Figure 2) matches the absorbance features of reduced $Fe(TPP)^{2-}$, which was independently generated by the parent compound Fe(TPP)Cl by *in situ* spectroelectrochemical UV-visible spectroscopy at the electrocatalytic potential (−2.35 V vs $[Fe(C_5H_5)_2]^{+/0}$, blue trace). Mass spectrometry of the postelectrolysis solution only had features corresponding to DPIy (Figure S19). We note that the mass spectrometry of DPICx alone also results in only DPIy, so the result indicates that there is no other decomposition of the NHC after electrolysis. However, the postelectrolysis solution was also characterized by ^{13}C NMR spectroscopy, with resonances corresponding to DPIy, indicating regeneration of the NHC (Figure S24).

https://doi.org/10.1021/jacs.4c18303
J. Am. Chem. Soc. 2025, 147, 16099−16106

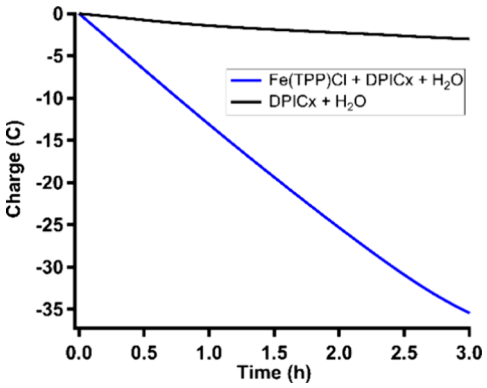

Figure 1. Controlled potential electrolysis (CPE) of 20 mM DPICx (black) with 1 mM Fe(TPP)Cl (blue) and 60 mM H_2O at −2.35 V vs $Fe(C_5H_5)_2^{+/0}$. CPE experiments were performed in THF with 0.1 M n-Bu_4NPF_6 on carbon cloth electrodes.

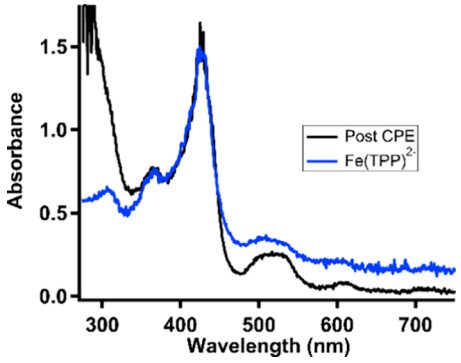

Figure 2. UV-visible spectra of 1 mM $Fe(TPP)^{2-}$ with 20 mM DPICx and 60 mM H_2O postelectrolysis (−2.35 V vs $Fe(C_5H_5)_2^{+/0}$, 4 h) (black) diluted 1:10 with THF and generated spectroelectrochemically (100 μM Fe(TPP)Cl, −2.35 V vs $Fe(C_5H_5)_2^{+/0}$) (blue). The features below 300 nm in the black trace correspond to DPIy and unreacted DPICx.

To test DPIy's competence as a sorbent, dilute CO_2 streams were passed through 20 mM solutions of DPIy in THF for 1 h to generate DPICx *in situ* for reduction, followed by an N_2 purge to eliminate free CO_2 as a competitive substrate (Figures S22−S26). Streams composed of 10:90 CO_2:N_2 were used to simulate flue gas concentrations. Electrolysis of these solutions with Fe(TPP)Cl results in similarly high Faradaic yields for CH_4 (92.5 ± 2.1%, Table 1). The use of a more dilute stream corresponding to direct air concentrations (0.04%) also displayed full conversion from DPIy to DPICx by ^{1}H and ^{13}C NMR spectroscopy, with high Faradaic yields of 94.5 ± 0.7% for CH_4 upon electrolysis. Similar to using DPICx as the starting material, the postelectrolysis analysis of *in situ* generated DPICx from DPIy and dilute CO_2 reveals regeneration of DPIy by ^{1}H NMR spectroscopy (Figure S22). A separate experiment described under mechanistic studies investigated the catalytic activity in the presence of both DPICx and CO_2.

To ensure that the product CH_4 stems from the CO_2 bound to the NHC, DPICx was synthesized *in situ* using DPIy and $^{13}CO_2$. The reaction with DPIy and $^{13}CO_2$ quantitatively produced DPI^{13}Cx as characterized by ^{13}C NMR spectroscopy (Figure S26). Following electrolysis, the analysis of the headspace by mass spectrometry confirms $^{13}CH_4$ as the gaseous product. Some formate is detected by ^{13}C NMR spectroscopy in the liquid phase (*vide infra*).

Mechanistic Studies. Cyclic voltammetry (CV) of Fe(TPP)Cl in the absence of substrates displays three cathodic features, as previously described and shown in Figure S1.[15] A quasi-reversible event at −0.6 V vs $[Fe(C_5H_5)_2]^{+/0}$ is assigned to the reduction of Fe(III) to Fe(II) followed by dissociation of the axial chloride ligand.[29] This reduction event is followed by two reversible one-electron reductions of the porphyrin ligand at −1.7 and −2.2 V vs $[Fe(C_5H_5)_2]^{+/0}$.[30] Under an atmosphere of CO_2 with a proton source such as water or phenol, the feature at −2.2 V vs $[Fe(C_5H_5)_2]^{+/0}$ exhibits a loss of reversibility and enhancement of the cathodic current that corresponds to electrocatalysis.[31] Electrolysis at this potential results in catalytic and quantitative CO_2 reduction to CO.[16]

In contrast to Fe(TPP)Cl under CO_2, the cyclic voltammogram with up to 10 equiv of DPICx exhibits no change to the third reduction event (Figure S2). Furthermore, the titration of the proton source (water) into the solution does not result in enhancement of the current, even at slow scan rates (25 mV/s), indicating that catalysis at the reduced complex is slow (<0.5 s^{-1}).[32] Controlled potential electrolysis of DPICx at −1.7 V vs $[Fe(C_5H_5)_2]^{+/0}$, which corresponds to the second reduction event, results in only the formation of $[Fe(TPP)]^-$ and no catalytic products (Table 1). Only CPE experiments performed at the third reduction event, where $[Fe(TPP)]^{2-}$ is formed, result in CH_4. Reduction at −2.7 V vs $[Fe(C_5H_5)_2]^{+/0}$, which corresponds to direct DPICx reduction, does not result in any gaseous products.

The lack of significant catalytic current in the cyclic voltammogram with DPICx as the substrate indicates that it is not as fast as the reduction of CO_2 under the same conditions. The difference in rate is illustrated in a substrate competition experiment. Electrolysis of Fe(TPP)Cl and a 20 mM DPICx solution under 1 atm of CO_2 (expected concentration of 200−210 mM)[33] for 2.8 h resulted in the exclusive production of CO as the primary product (quantitative Faradaic efficiency for CO), indicating that CO_2 reduction is faster than DPICx reduction (Figure S11). When free CO_2 is purged from the system by using N_2 to leave only DPICx as the substrate, product selectivity returns to CH_4 upon electrolysis.

The lack of changes in the cyclic voltammogram at $Fe(TPP)Cl^{-1/-2}$ reduction with excess DPICx indicates that there are no significant interactions between the active catalyst and substrate (Figure S2). Spectroelectrochemical UV-visible spectra were collected immediately after reduction of Fe(TPP)Cl at −2.35 V vs $Fe(C_5H_5)_2^{+/0}$ under catalytic conditions (20 mM DPICx, 60 mM H_2O). The only metal-based species observed was the reduced compound $[Fe(TPP)]^{2-}$ (Figure 2). These results indicate that a metal-based intermediate upon reduction of the catalyst is short-lived or is only present at a low concentration under catalytic conditions.

As metal-based intermediates are not detected spectroscopically, we used computational methods to investigate the interaction between DPICx and the $Fe(TPP)^{2-}$ catalyst as well as reduced derivatives. A potential of −2.35 V[34] vs $Fe(C_5H_5)_2^{+/0}$ was modeled.[35] Since the water content of THF changes during catalysis and the pH is inexact, the chemical potential for protons was chosen to render protonation of DPIy thermoneutral (observed by NMR spectroscopy to be unprotonated following catalysis). For iron compounds, multiplicities up to quintet were optimized,

https://doi.org/10.1021/jacs.4c18303
J. Am. Chem. Soc. 2025, 147, 16099−16106

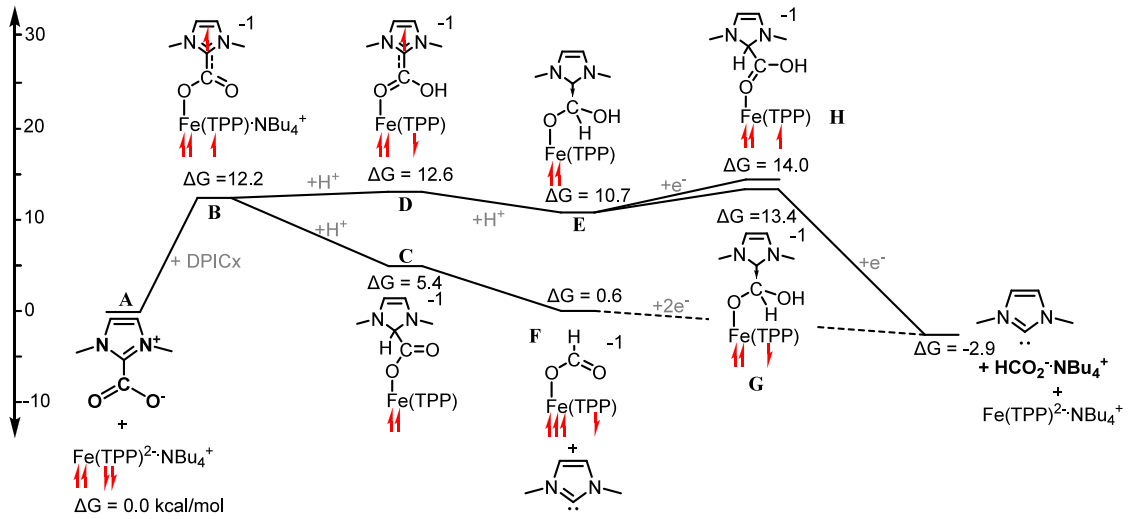

Figure 3. Potential intermediates in the reduction of DPICx to formate catalyzed by $Fe(TPP)^{2-}$. The total spin and approximate localization of unpaired electrons are denoted by red arrows. Diisopropylphenyl groups have been omitted for clarity. Formate is the only experimentally observed C1 intermediate prior to the product CH_4 and is only observed by ^{13}C NMR when ^{13}C-labeled DPICx is used.

Scheme 1. Potential Substrate Intermediates, Assuming That the Sorbent-CO_2 Bond Is Retained Throughout Reduction (Top) or Cleaved Early to Form the Product (Bottom)[a]

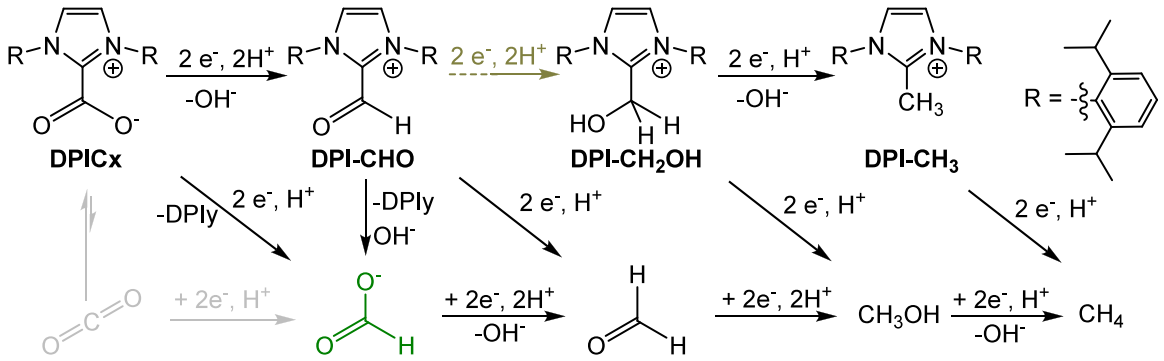

[a]The gray CO_2 intermediate is not expected to be present because of the strong binding to NHC and because it is never detected under experimental conditions. All black and green intermediates have been tested as substrates under catalytic conditions except DPI-CHO, which could not be isolated (products and Faradaic efficiencies are shown in Table 1). The green intermediate is also detected under catalytic conditions.

and a broken-symmetry singlet or doublet was sought. The lowest energy state among these is reported. The ground state determined for $Fe(TPP)^{2-}$ was as described previously by Neese et al.: S=0 with a doubly occupied, axial d_z^2 orbital and single electrons in the d_{xz} and d_{yz} orbitals, each antiferromagnetically coupled to an electron in an overlapping porphyrin p orbital.[30] Iron in this state presents a nucleophilic site to potential ligands, so Cl^- is lost from (TPP)FeCl upon reduction, and calculations showed that THF and the DPIy carbon do not bond to $Fe(TPP)^{2-}$. A pattern emerged for intermediates including a Fe−O bond: the iron center preferred a "local" triplet configuration (i.e., approximately two electrons of spin density on iron), while any additional electrons on the (TPP)Fe fragment were distributed over the macrocycle. The relative energies of intermediates and spin states will be dependent on the functional employed. In THF, the binding energy of 1 atm CO_2 to 1 M DPIy was calculated to be −5.1 kcal/mol, which is close to the −4.5 kcal/mol value previously calculated in DMSO, although the prior work used the conditions of 1 M CO_2.[6] We computed the coordination of DPICx to $Fe(TPP)^{2-}$ to be endergonic by 12 kcal/mol (Figure 3). Notably, coordination includes an electronic rearrangement in which one electron from the porphyrin ring is transferred to and delocalized over the imidazolium carboxylate p-system. The lack of changes in the spectroelectrochemical UV-visible spectra for *in situ* generated $Fe(TPP)^{2-}$ in the presence of DPICx is consistent with the high free energy associated with this interaction.

We examined proposed intermediates generated by the sequential addition of protons and electrons, which lead exergonically to formate, free carbene, and regenerated $Fe(TPP)^{2-}$ (Figure 3).[36] One thermodynamically reasonable pathway involves the addition of two protons to generate intermediate **E**, a formic acid molecule bound by a frustrated Lewis acid−base pair (comprising the carbene and an Fe^{II} cation). The two electrons that were initially located on the porphyrin are localized in the new C−H bond of this intermediate. Decomposition of this complex, either before (via **F**) or after (via **G**) a one-electron reduction, leads to products. Another pathway leads from **B** via the protonation of the imidazolium carbon to **C**. Protonation of **C** (or a water-catalyzed rearrangement) and dissociation of the carbon−carbon bond lead to liberated carbene and a $Fe(TPP)(OCHO)^{-1}$ complex.

https://doi.org/10.1021/jacs.4c18303
J. Am. Chem. Soc. 2025, 147, 16099−16106

Instead of C−C bond dissociations, which would liberate formate, these intermediates may lead directly to the further reduction of DPICx. Protonolysis of the C−OH bond in **E** or **G** may compete with the liberation of formate, while **F** could allow free formate to enter the reaction as a reactant itself, as observed (*vide infra*).

We used additional experiments to gain further understanding of the viable C-based intermediates for the 8 e^- reduction, as shown in Scheme 1. The top row corresponds to a mechanism in which the sorbent-CO_2 bond is retained throughout most of the reduction, while the second row corresponds to early cleavage of the sorbent-CO_2 bond followed by reduction of the subsequent C1 species to CH_4. Reduction products were detected by GC, and only CH_4 or H_2 was observed. The ^{1}H NMR spectra were examined for C1 products, but none were detected.

Among the potential C-based intermediates that retain the sorbent-CO_2 bond (top row), DPI-CH_2OH and DPI-CH_3 were successfully isolated (Synthesis and Characterization section in the Supporting Information). These potential intermediates were studied for their competence as substrates for electrocatalytic reduction by Fe(TPP)Cl under the same conditions as those that produce CH_4 with DPICx. Electrolysis of the 4 e^- reduced species, DPI-CH_2OH, displayed little conversion to methane (FE = 11.3%). The final NHC-based intermediate DPI-CH_3 generated on average 17% FE for methane; however, there was also significant hydrogen evolution (∼52%) and background contribution of methane (FE = 8.8% in the absence of an iron catalyst). Attempts to isolate the aldehyde (DPI-CHO) by oxidation of DPI-CH_2OH were unsuccessful due to the formation of protonated DPIy (H-DPIy).[37] A prior study proposed that water or hydroxide can react with NHC-aldehyde complexes to release formic acid and free carbene.[38] As a result, we believe that if DPI-CHO is formed, then it can react further under catalytic conditions to produce formate and DPIy.

The potential C1 intermediates (second row, Scheme 1) were also tested as substrates for electrocatalytic reduction by Fe(TPP)Cl under the same conditions (Figures S5−S7). With a calculated free energy of −5 kcal/mol for CO_2 binding to DPIy,[6] we expect negligible dissociation of CO_2 from DPICx, which is confirmed experimentally. DPICx is stable in solution by ^{1}H NMR spectroscopy even after purging with N_2. Additionally, CO, the terminal product of the reduction of CO_2 with Fe(TPP)Cl, is not observed from electrolysis, which excludes CO_2 as a potential substrate (gray, Scheme 1).

Formate, formaldehyde, and methanol were also tested as substrates under electrocatalytic conditions, and the resulting Faradaic efficiencies for the products are shown in Table 1. Formic acid was also tested, although we expect only that the formate species will be present under the weakly acidic catalytic conditions. These CPE experiments demonstrate that these C1 intermediates all lead to methane, albeit with lower Faradaic efficiencies than DPICx. The CH_4 observed with formic acid may be from the generation of formate upon hydrogen evolution. These intermediates are not detected under catalytic conditions when DPICx is the substrate (except for formate when the ^{13}C-labeled compound is used), so we expect their concentrations during DPICx reduction to be very low. In contrast, these CPEs of potential intermediates were performed at a concentration of 20 mM, which may explain the lower overall Faradaic efficiencies for CH_4. Other intermediates may also play a role in facilitating catalysis but are not present in these experiments. For example, these experiments did not contain DPICx or DPIy. However, they demonstrate whether a viable chemical path exists for their reduction to CH_4. Corresponding electrolysis experiments without a catalyst were performed at the same potential (at −2.35 V vs $Fe(C_5H_5)_2^{+/0}$) and led to minimal direct reduction of these substrates at the electrode, except for formic acid, which led to substantial hydrogen production. Similar to the case when DPICx is used as the substrate, $[Fe(TPP)]^{2-}$ is typically observed after electrolysis, which may account for some of the charge passed. The current versus time traces for these controlled potential electrolyses are shown in Figures S10−S15.

As mentioned previously, when isotopically labeled $^{13}CO_2$ was used to generate the DPICx substrate, formate ($H^{13}CO_2^-$) was detected in the ^{13}C NMR spectrum along with $^{13}CH_4$, indicating that it is a possible intermediate. This observation, along with the comparatively high Faradaic efficiency for CH_4 when it is a substrate (68.6 ± 6.2%), provides evidence for early cleavage of the sorbent-CO_2 bond, which is an accessible pathway in the calculation with $Fe(TPP)^{2-}$. Formate can result from the direct reduction of DPICx to form DPI-CHO, followed by addition of hydroxide and subsequent decarboxylation to form formate and DPIy. Alternatively, reduction of DPICx can result in the concurrent formation of DPIy and formate. The lack of detection by ^{1}H and ^{13}C NMR spectroscopy of the DPI-CH_2OH and DPI-CH_3 intermediates, combined with the poor yields for methane, indicates that the intermediates in the top row are less likely.

DISCUSSION

The interaction between NHC and CO_2 plays a key role in its reduction by Fe(TPP)Cl. This interaction is expected to impact the reactivity from the very first catalytic steps with $Fe(TPP)^{2-}$. A prior calculation resulted in a free energy change (ΔG) of 2.5 kcal/mol for binding CO_2 to $Fe(TPP)^{2-}$ to form a metal carboxylate.[39] The Brønsted basic iron carboxylate is then protonated twice to initiate cleavage of the C−O bond, release water, and give a CO ligand. In DPICx, the interaction of the NHC at the carbon in CO_2 precludes the equivalent interaction with the metal so that the iron carboxylate cannot form. Instead, our calculation indicates binding of DPICx to the same $Fe(TPP)^{2-}$ species via the anionic oxygen with a free energy change of 12 kcal/mol (Figure 3) compared to the 2.5 kcal/mol calculated for CO_2. This change leads to an unfavorable pre-equilibrium for substrate binding, which may partially explain the slower rate of DPICx reduction. This disparity is not unexpected; the filled d_{z^2} orbital of $Fe(TPP)^{2-}$ can interact more favorably with the lowest unoccupied molecular orbital (LUMO) of CO_2 than the carboxylate in DPICx. Coordination of DPICx to $Fe(TPP)^{2-}$ includes electron transfer to the DPICx ligand, which results in the nucleophilic iron center becoming Lewis acidic and coordinating the Lewis basic oxygen. While calculated free energies for DPICx binding and other potential intermediates in Figure 3 are higher than that of $Fe(TPP)^{2-}$, they are accessible in a reaction that is slow at room temperature, which is consistent with experimental results. Interestingly, CH_4 was also observed as the product when DPICx was used as the substrate with another CO_2-to-CO electrocatalyst, $Ni(cyclam)^{2+}$.[12] When CO_2 is the substrate, the Ni active site is believed to interact similarly to make a metal carboxylate. These catalysts may have similar mechanistic pathways with DPICx as the substrate.

https://doi.org/10.1021/jacs.4c18303
J. Am. Chem. Soc. 2025, 147, 16099−16106

As previously noted, Fe(TPP)Cl exclusively generates CO as the terminal product when CO_2 is the substrate under analogous conditions. The only exception is a cleverly designed Fe porphyrin derivative that contains a secondary sphere functionality to stabilize the CO substrate at the metal, resulting in the electrocatalytic reduction of CO to CH_4.[23] Additionally, the photolytic reduction of CO_2 to CH_4 with related Fe porphyrin-based catalysts is proposed to proceed through a CO intermediate.[24] However, we do not believe that CO is an intermediate in this system because it is never detected in the headspace by GC and is not expected to bind to $Fe(TPP)^{2-}$ sufficiently for further reduction based on prior studies with this catalyst for CO_2R.[15,16]

Our mechanistic studies indicate that formate is a likely C1 intermediate. A Fe(TPP)Cl catalyst was reported that reduces CO_2 to formate with the addition of tertiary amines. The amines are believed to bind to the reduced $Fe(TPP)^{2-}$ complex and increase the basicity of the resulting metal carboxylate, leading to protonation to form formate.[40] The analogous metal carboxylate intermediate is not accessible with the DPICx substrate; however, we examined the possibility of interactions of DPIy with the metal complexes. Spectroelectrochemical UV-visible experiments with 20 equiv of DPIy and $Fe(TPP)^{2-}$ generated *in situ* exhibit a small reduction in the spectra of $Fe(TPP)^{2-}$, indicating some interaction with DPIy (Figure S21). However, it is unclear whether this species is associated with catalysis, as there is no DPIy present when catalysis is initiated. The features associated with DPIy and $Fe(TPP)^{2-}$ are also not present in the postelectrolysis UV-visible spectra (Figure 2). While DPIy may interact with $Fe(TPP)^{2-}$, we do not believe it inhibits catalysis. We do not see any reduction in catalytic activity after multiple turnovers even as the concentration of DPIy is increasing.

CONCLUSIONS

These studies indicate that DPIy is an effective sorbent for the capture of dilute CO_2 and a catalytic auxiliary. The resulting captured-CO_2 species, DPICx, is activated toward electrocatalytic reduction with Fe(TPP)Cl to produce CH_4 at high Faradaic efficiencies with regeneration of the sorbent DPIy. Furthermore, water is used as the proton source, indicating that this process can be coupled to renewable electricity to generate carbon-neutral methane. From our studies, it appears that the NHC activates the CO_2 toward the 2 e^- reduced product formate, which is then reduced further under these conditions to CH_4. All potential C1 intermediates (HCO_2^-, HCHO, and CH_3OH) give CH_4 as the major carbon product.

The success of a carbene for this purpose is particularly exciting, as it is a modular platform that can tune CO_2 activation through both σ- and π-interactions to influence subsequent reactivity. These interactions can be controlled through electronic and steric effects.[5,7]

These results have broader implications toward integrating CO_2 capture and conversion. CO_2 has unique interactions with a broad spectrum of sorbents. These interactions can be fine-tuned to pair with catalytic systems to guide the product selectivity. In this way, new systems can be developed that both capture CO_2 from dilute streams and result in products that would otherwise not be accessible with CO_2 substates. These efforts are critical for reducing the cost and improving the efficiency of the utilization of CO_2 from the source to the product.

ASSOCIATED CONTENT

Supporting Information

The Supporting Information is available free of charge at https://pubs.acs.org/doi/10.1021/jacs.4c18303.

General experimental methods, physical methods, Faradaic efficiency calculations, electrochemical data, NMR spectroscopic data, synthesis and characterization, and computational methods (PDF)

TXT file of the terms used in this work (TXT)

AUTHOR INFORMATION

Corresponding Authors

Robert J. Nielsen − *Department of Chemical and Biomolecular Engineering, University of California, Irvine, Irvine, California 92697, United States*; Email: rjnielse@uci.edu

Jenny Y. Yang − *Department of Chemistry, University of California, Irvine, Irvine, California 92697, United States*; orcid.org/0000-0002-9680-8260; Email: j.yang@uci.edu

Authors

Jared S. Stanley − *Department of Chemistry, University of California, Irvine, Irvine, California 92697, United States*

Hunter N. Pauker − *Department of Chemical and Biomolecular Engineering, University of California, Irvine, Irvine, California 92697, United States*

Erin Kuker − *Department of Chemistry, University of California, Irvine, Irvine, California 92697, United States*

Vy Dong − *Department of Chemistry, University of California, Irvine, Irvine, California 92697, United States*; orcid.org/0000-0002-8099-1048

Complete contact information is available at: https://pubs.acs.org/10.1021/jacs.4c18303

Author Contributions

The manuscript was written through contributions of all authors. All authors have given approval to the final version of the manuscript.

Funding

This work was supported as part of the Center for Closing the Carbon Cycle, an Energy Frontier Research Center funded by the U.S. Department of Energy, Office of Science, Basic Energy Sciences under award number DE-SC0023427.

Notes

The authors declare no competing financial interest.

ACKNOWLEDGMENTS

We wish to thank the UCI Mass Spectrometry Facility for assistance with gas chromatography measurements on an Agilent 7890b GC. This work was supported as part of the Center for Closing the Carbon Cycle, an Energy Frontier Research Center funded by the U.S. Department of Energy, Office of Science, Basic Energy Sciences under award number DE-SC0023427.

REFERENCES

(1) Balamurugan, M.; Merakeb, L.; Nam, K. T.; Robert, M. Electrochemical CO_2 Reduction. In *Chemical Valorisation of Carbon Dioxide*, Stefanidis, G.; Stankiewicz, A. Eds.; Royal Society of Chemistry, 2022; p 1804.

(2) Francke, R.; Schille, B.; Roemelt, M. Homogeneously Catalyzed Electroreduction of Carbon Dioxide—Methods, Mechanisms, and Catalysts. *Chem. Rev.* **2018**, *118* (9), 4631−4701.
(3) Deutsch, T. G.; Baker, S.; Agbo, P.; Kauffman, D. R.; Vickers, J.; Schaidle, J. A. *Summary Report of the Reactive CO2 Capture: Process Integration for the New Carbon Economy Workshop, February 18-19, 2020*. 2020. https://www.nrel.gov/docs/fy21osti/78466.pdf (accessed 05/01/2024).
(4) Freyman, M. C.; Huang, Z.; Ravikumar, D.; Duoss, E. B.; Li, Y.; Baker, S. E.; Pang, S. H.; Schaidle, J. A. Reactive CO2 capture: A path forward for process integration in carbon management. *Joule* **2023**, *7* (4), 631−651.
(5) Van Ausdall, B. R.; Glass, J. L.; Wiggins, K. M.; Aarif, A. M.; Louie, J. A Systematic Investigation of Factors Influencing the Decarboxylation of Imidazolium Carboxylates. *Journal of Organic Chemistry* **2009**, *74* (20), 7935−7942.
(6) Wang, Z.; Xue, X.-S.; Fu, Y.; Ji, P. Comprehensive Basicity Scales for N-Heterocyclic Carbenes in DMSO: Implications on the Stabilities of N-Heterocyclic Carbene and CO2 Adducts. *Chem. − Asian J.* **2020**, *15* (1), 169−181.
(7) Luca, O. R.; Fenwick, A. Q. Organic reactions for the electrochemical and photochemical production of chemical fuels from CO2 − The reduction chemistry of carboxylic acids and derivatives as bent CO2 surrogates. *Journal of Photochemistry and Photobiology B: Biology* **2015**, *152*, 26−42.
(8) Lee, G.; Li, Y. C.; Kim, J.-Y.; Peng, T.; Nam, D.-H.; Sedighian Rasouli, A.; Li, F.; Luo, M.; Ip, A. H.; Joo, Y.-C.; et al. Electrochemical upgrade of CO2 from amine capture solution. *Nature Energy* **2021**, *6* (1), 46−53.
(9) Zhou, H.; Zhang, W.-Z.; Liu, C.-H.; Qu, J.-P.; Lu, X.-B. CO2 Adducts of N-Heterocyclic Carbenes: Thermal Stability and Catalytic Activity toward the Coupling of CO2 with Epoxides. *Journal of Organic Chemistry* **2008**, *73* (20), 8039−8044.
(10) Saptal, V. B.; Gade, S. M.; Vilé, G.; Walkowiak, J.; Bhanage, B. M.; Organocatalytic Reductive Functionalization of Carbon Dioxide. In *Sustainable Utilization of Carbon Dioxide: From Waste to Product*, Jawaid, M.; Khan, A. Eds.; Springer Nature Singapore, 2023; pp 1−36.
(11) Stiernet, P.; Pang, B.; Taton, D.; Yuan, J. The promise of N-heterocyclic carbenes to capture and valorize carbon dioxide. *Sustainable Chemistry for Climate Action* **2023**, *2*, No. 100018.
(12) Luca, O. R.; McCrory, C. C. L.; Dalleska, N. F.; Koval, C. A. The Selective Electrochemical Conversion of Preactivated CO2 to Methane. *J. Electrochem. Soc.* **2015**, *162* (7), H473.
(13) Gurkan, B.; Goodrich, B. F.; Mindrup, E. M.; Ficke, L. E.; Massel, M.; Seo, S.; Senftle, T. P.; Wu, H.; Glaser, M. F.; Shah, J. K.; et al. Molecular Design of High Capacity, Low Viscosity, Chemically Tunable Ionic Liquids for CO2 Capture. *J. Phys. Chem. Lett.* **2010**, *1* (24), 3494−3499.
(14) Matsubara, Y.; Grills, D. C.; Kuwahara, Y. Thermodynamic Aspects of Electrocatalytic CO2 Reduction in Acetonitrile and with an Ionic Liquid as Solvent or Electrolyte. *ACS Catal.* **2015**, *5* (11), 6440−6452.
(15) Hammouche, M.; Lexa, D.; Savéant, J. M.; Momenteau, M. Catalysis of the electrochemical reduction of carbon dioxide by iron("0") porphyrins. *Journal of Electroanalytical Chemistry and Interfacial Electrochemistry* **1988**, *249* (1), 347−351.
(16) Costentin, C.; Robert, M.; Savéant, J.-M. Current Issues in Molecular Catalysis Illustrated by Iron Porphyrins as Catalysts of the CO2-to-CO Electrochemical Conversion. *Acc. Chem. Res.* **2015**, *48* (12), 2996−3006.
(17) Cai, J.; Zhao, Q.; Hsu, W.-Y.; Choi, C.; Liu, Y.; Martirez, J. M. P.; Chen, C.; Huang, J.; Carter, E. A.; Huang, Y. Highly Selective Electrochemical Reduction of CO2 into Methane on Nanotwinned Cu. *J. Am. Chem. Soc.* **2023**, *145* (16), 9136−9143.
(18) Pan, H.; Barile, C. J. Electrochemical CO2 reduction to methane with remarkably high Faradaic efficiency in the presence of a proton permeable membrane. *Energy Environ. Sci.* **2020**, *13* (10), 3567−3578.
(19) Han, L.; Song, S.; Liu, M.; Yao, S.; Liang, Z.; Cheng, H.; Ren, Z.; Liu, W.; Lin, R.; Qi, G.; et al. Stable and Efficient Single-Atom Zn Catalyst for CO2 Reduction to CH4. *J. Am. Chem. Soc.* **2020**, *142* (29), 12563−12567.
(20) Qiu, Y.-L.; Zhong, H.-X.; Zhang, T.-T.; Xu, W.-B.; Li, X.-F.; Zhang, H.-M. Copper Electrode Fabricated via Pulse Electrodeposition: Toward High Methane Selectivity and Activity for CO2 Electroreduction. *ACS Catal.* **2017**, *7* (9), 6302−6310.
(21) Ahmed, M. E.; Adam, S.; Saha, D.; Fize, J.; Artero, V.; Dey, A.; Duboc, C. Repurposing a Bio-Inspired NiFe Hydrogenase Model for CO2 Reduction with Selective Production of Methane as the Unique C-Based Product. *ACS Energy Letters* **2020**, *5* (12), 3837−3842.
(22) Nganga, J. K.; Wolf, L. M.; Mullick, K.; Reinheimer, E.; Saucedo, C.; Wilson, M. E.; Grice, K. A.; Ertem, M. Z.; Angeles-Boza, A. M. Methane Generation from CO2 with a Molecular Rhenium Catalyst. *Inorg. Chem.* **2021**, *60* (6), 3572−3584.
(23) Patra, S.; Bhunia, S.; Ghosh, S.; Dey, A. Outer-Coordination-Sphere Interaction in a Molecular Iron Catalyst Allows Selective Methane Production from Carbon Monoxide. *ACS Catal.* **2024**, *14* (10), 7299−7307.
(24) Rao, H.; Schmidt, L. C.; Bonin, J.; Robert, M. Visible-light-driven methane formation from CO2 with a molecular iron catalyst. *Nature* **2017**, *548* (7665), 74−77.
(25) Kumagai, H.; Nishikawa, T.; Koizumi, H.; Yatsu, T.; Sahara, G.; Yamazaki, Y.; Tamaki, Y.; Ishitani, O. Electrocatalytic reduction of low concentration CO2. *Chemical Science* **2019**, *10* (6), 1597−1606.
(26) Miyaji, M.; Tamaki, Y.; Kamogawa, K.; Abiru, Y.; Abe, M.; Ishitani, O. CO2 Capture and Electrochemical Reduction of Low-Concentration CO2 Using a Re(I)-Complex Catalyst in Ethanol. *ACS Catal.* **2024**, *14* (13), 10403−10411.
(27) Bhattacharya, M.; Sebghati, S.; VanderLinden, R. T.; Saouma, C. T. Toward Combined Carbon Capture and Recycling: Addition of an Amine Alters Product Selectivity from CO to Formic Acid in Manganese Catalyzed Reduction of CO2. *J. Am. Chem. Soc.* **2020**, *142* (41), 17589−17597.
(28) Sampaio, R. N.; Grills, D. C.; Polyansky, D. E.; Szalda, D. J.; Fujita, E. Unexpected Roles of Triethanolamine in the Photochemical Reduction of CO2 to Formate by Ruthenium Complexes. *J. Am. Chem. Soc.* **2020**, *142* (5), 2413−2428.
(29) Lexa, D.; Momenteau, M.; Mispelter, J. Characterization of the reduction steps of Fe(III) porphyrins. *Biochimica et Biophysica Acta (BBA) - General Subjects* **1974**, *338* (1), 151−163.
(30) Römelt, C.; Song, J.; Tarrago, M.; Rees, J. A.; van Gastel, M.; Weyhermüller, T.; DeBeer, S.; Bill, E.; Neese, F.; Ye, S. Electronic Structure of a Formal Iron(0) Porphyrin Complex Relevant to CO2 Reduction. *Inorg. Chem.* **2017**, *56* (8), 4745−4750.
(31) Costentin, C.; Drouet, S.; Passard, G.; Robert, M.; Savéant, J.-M. Proton-Coupled Electron Transfer Cleavage of Heavy-Atom Bonds in Electrocatalytic Processes. Cleavage of a C−O Bond in the Catalyzed Electrochemical Reduction of CO2. *J. Am. Chem. Soc.* **2013**, *135* (24), 9023−9031.
(32) Appel, A. M.; Pool, D. H.; O'Hagan, M.; Shaw, W. J.; Yang, J. Y.; Rakowski DuBois, M.; DuBois, D. L.; Bullock, R. M. [Ni(PPh2NBn2)2(CH3CN)]2+ as an Electrocatalyst for H2 Production: Dependence on Acid Strength and Isomer Distribution. *ACS Catal.* **2011**, *1* (7), 777−785.
(33) Gennaro, A.; Isse, A. A.; Vianello, E. Solubility and electrochemical determination of CO2 in some dipolar aprotic solvents. *Journal of Electroanalytical Chemistry and Interfacial Electrochemistry* **1990**, *289* (1), 203−215.
(34) Connelly, N. G.; Geiger, W. E. Chemical Redox Agents for Organometallic Chemistry. *Chem. Rev.* **1996**, *96* (2), 877−910. Assuming a 800mV potential difference between the standard hydrogen electrode and Fe(C5H5)2+/0 in THF as stated in
(35) Geometries and solvated electronic energies were computed with TPSS0-D3(BJ) functional; def2-TZVP(-f) basis augmented with diffuse function and the Los Alamos pseudopotential for Fe complemented by a 3z+f valence set; continuum solvation representing THF via the SMD model.

https://doi.org/10.1021/jacs.4c18303
J. Am. Chem. Soc. 2025, 147, 16099−16106

(36) The free energies of the iron complexes are uncertain beyond the usual error of DFT due to the solvation of charged species in the low-dielectric solvent THF. We have included an explicit NBu4+ cation in each model which would otherwise carry a charge of −2.
(37) Xin, H.; Zhu, X.; Yan, H.; Song, X. Revelation from the Reaction of 1,4-Diazabutadiene with Perchloric Acid: An Approach to the Synthesis of Imidazolium Perchlorates. *J. Heterocycl. Chem.* **2016**, *53* (5), 1363−1366.
(38) Xin, H.-X.; Liu, Q.; Yan, H.; Song, X.-Q. Stability and decarbonylation of 1,3-dialkyl-2-formylimidazolium perchlorate in solution. *Can. J. Chem.* **2013**, *91* (6), 442−447.
(39) Tarrago, M.; Ye, S.; Neese, F. Electronic structure analysis of electrochemical CO2 reduction by iron-porphyrins reveals basic requirements for design of catalysts bearing non-innocent ligands. *Chemical Science* **2022**, *13* (34), 10029−10047.
(40) Margarit, C. G.; Asimow, N. G.; Costentin, C.; Nocera, D. G. Tertiary Amine-Assisted Electroreduction of Carbon Dioxide to Formate Catalyzed by Iron Tetraphenylporphyrin. *ACS Energy Letters* **2020**, *5* (1), 72−78.

https://doi.org/10.1021/jacs.4c18303
J. Am. Chem. Soc. 2025, 147, 16099−16106